Journal of Geochemical Exploration 177 (2017) 61–72

Contents lists available at ScienceDirect

Journal of Geochemical Exploration

journal homepage: www.elsevier.com/locate/gexplo

Petrogeochemical assessment of rock units and identification of alteration/mineralization indicators using portable X-ray fluorescence measurements: Applications to the Fire Tower Zone (W-Mo-Bi) and the North Zone (Sn-Zn-In), Mount Pleasant deposit, New Brunswick, Canada

Wei Zhang [a,b,*], David R. Lentz [b], Brittany E. Charnley [c]

[a] MLR Key Laboratory of Metallogeny and Mineral Assessment, Institute of Mineral Resources, CAGS, Beijing, 100037, China
[b] Department of Earth Sciences, University of New Brunswick, Fredericton, N.B. E3B 5A3, Canada
[c] Geological Surveys Branch, New Brunswick Department of Energy and Mines, Fredericton, N.B., E3B 5A3, Canada

ARTICLE INFO

Article history:
Received 3 May 2016
Revised 16 January 2017
Accepted 26 February 2017
Available online 1 March 2017

Keywords:
pXRF
Immobile elements
PCA
Lithogeochemistry
Mount Pleasant deposit

ABSTRACT

The Mount Pleasant polymetallic deposits are located along the southwestern margin of the Late Devonian Mount Pleasant Caldera Complex in southwestern New Brunswick, Canada. The Fire Tower Zone (W-Mo-Bi) and the North Zone (Sn-Zn-In) comprise the main mineralized zones within the Mount Pleasant deposit. The rock units examined at surface in both zones are highly altered and are surface weathered to some extent. In order to classify these rock units with confidence, the Olympus X-5000 portable X-ray Fluorescence (pXRF) spectrometer was used in this study to rapidly obtain the geochemical composition of these rocks, identify lithologic discriminants, and find alteration/mineralization indicators in these areas. The immobile elements Ti, Zr, Nb, Y, and Th were selected to discriminate among various rock types. The Little Mount Pleasant Formation has the highest Ti and Zr and the Mount Pleasant Granitic Suite (MPGS, GI and GII) contains the highest Y, Nb, and Th. The McDougall Brook Granitic Suite (MBGS) has an intermediate composition between them. The element ratios of Zr/Ti, Nb/Ti, Y/Ti, and Th/Ti effectively discriminate these rock units and increase from the Little Mount Pleasant Formation, to the MBGS, and then to the MPGS.

Greisen and propylitic alteration are reflected by strong depletion of K and Rb in some samples. The Fe and Mn typically are leached out of the mineralization system during the greisen alteration. Principal component analysis (PCA) was performed on the pXRF datasets. The first principal component (PC1) of the pXRF data from both the Fire Tower Zone and the North Zone mainly extracts information on Ti, Zr, Ce, Cr, V, Nb, Y, U, and Th, and thus represents different rock units. The PC2 is characterized by high-positive loadings of K, Rb, Fe, and Mn and negative loading of As and Mo. It is interpreted as the W-Mo mineralization indicator showing by the enrichment in Mo and depletion of K, Rb, Fe, and Mn associated with quartz + topaz + sericite + fluorite alteration. The PC3 consists of positive loadings of Sn, Zn, Cu, and S and slightly negative loadings of Sr and Ba, and thus represents the Sn-Zn mineralization in this area.

1. Introduction

Portable X-ray fluorescence (pXRF) spectrometers are widely used in mining and exploration programs, because they provide the advantage of completing measurements in situ (non-destructive) and collecting large amounts of geochemical data rapidly at low costs (Fisher et al., 2014). Although pXRF is considered a routine semi-quantitative analytical tool (Arne et al., 2014), the quality of pXRF data could be improved by rigorous calibration methods developed by Hall et al. (2014), Gazley et al. (2011a, 2011b), and Fisher et al. (2014). Vaillant et al. (2014) used the pXRF to acquire Cr, Ni, and Ti data to effectively explore for komatiite-hosted nickel sulphide deposits. Gazley et al. (2011a) investigated the Au/As ratios of rocks by pXRF to define different geochemical domains of Au mineralization. Coupled with preliminary metallurgical testing the pXRF dataset would attribute metallurgical performance to predict metallurgical recovery in different ore blocks. Ross et al. (2014) and Fisher et al. (2014) used the pXRF to detect the lithogeochemical variations of rock units and identify stratigraphic sequences.

The Mount Pleasant granite-related polymetallic (W-Mo-Bi in the Fire Tower Zone and Sn-Zn-In in the North Zone) deposit, located on the southwestern margin of the Late Devonian Mount Pleasant Caldera Complex in southwestern New Brunswick, Canada (Thorne et al., 2013).

* Corresponding author at: MLR Key Laboratory of Metallogeny and Mineral Assessment, Institute of Mineral Resources, CAGS, Beijing, 100037, China
E-mail address: wei.z@unb.ca (W. Zhang).

http://dx.doi.org/10.1016/j.gexplo.2017.02.005
0375-6742/

This Caldera Complex constitutes a sequence of Upper Devonian volcanic and sedimentary rocks, intruded by subvolcanic-plutonic rocks. Brittle deformation affected the rocks within parts of the caldera (Inverno and Hutchinson, 2006). The ore deposits occur within hydrothermal veins (lodes) and breccias associated with the Mount Pleasant Granitic Suite (MPGS, from oldest to youngest classified as Granites I, II, and III). The W-Mo-Bi mineralization is associated with Granite I and mainly occurs in the Fire Tower Zone (Kooiman et al., 1986). The tin deposits and other base metal (In-Cu-Zn) are associated with Granite II and are predominately in the North Zone (Sinclair et al., 1988). The Granite III might have potential for significant tin mineralization in its endogranitic setting (Inverno and Hutchinson, 2006). Therefore, the correct indentification of protolith distribution could provide important information for guiding exploration. However high degrees of alteration associated with mineralizing processes in this area make protolith recognition difficult (cf. Govett and Atherden, 1988). Conventional XRF methods used to analyse pulverized breccia samples provide the geochemical signature for a mixture of rock fragments in the breccia and the groundmass. The rock fragments may be from different sources, thus, in situ pXRF analysis, which can avoid obtaining mixed compositions, was used in this study and its data quality has been proved to be sufficient to improve lithological discrimination and exploration (Piercey and Devine, 2014). This is supplementary work to the analysis of Charnley and Lentz (2015) and Zhang and Lentz (2016). New calibration methods and principal component analysis were conducted in order to obtain more precise geochemical information and investigate variations of element contents in these rocks during alteration and mineralization processes.

2. Geological setting

The regional geology of the Mount Pleasant area has been described in detail by Kooiman et al. (1986), McCutcheon (1990), McCutcheon et al. (1997), Yang et al. (2003), Inverno and Hutchinson (2006), Sinclair et al. (2006), and most recently by Thorne et al. (2013). The Mount Pleasant deposit occurs along the southwest margin of the Mount Pleasant Caldera, which is an epicontinental-type caldera exposed over an area of 17 by 13 km (Fig. 1). To the north, the caldera rocks are overlain disconformably by sandstone and conglomerate of Middle Mississippian and Pennsylvanian strata of the Maritimes Basin (McCutcheon, 1990). To other directions, the caldera complex is bounded by the polydeformed Ordovician and Silurian turbiditic metasedimentary rocks. Generally the caldera rocks overlie older rocks unconformably, but in places, they appear to be in fault contact (Fig. 1). Rocks related to the Mount Pleasant Caldera were divided into exocaldera, intracaldera, and late caldera-fill sequences in order to reflect their depositional setting in relation to the volcanic architecture. Characteristics of each rock units are briefly summarized here and see McCutcheon (1990) and McCutcheon et al. (1997) for more details (Fig. 1).

The exocaldera sequence, in ascending stratigraphic order, is comprised of massive to amygdaloidal basalt and aphyric to plagioclase-phyric basalt underlain by rhyolitic crystal tuff and lithic tuff, and minor reddish polymictic conglomerate (the Hoyt Station Basalt); a sequence of ash flows with overlying reddish brown mudstone (the Rothea Formation); plagioclase phyric and amygdaloidal andesite flows, and brecciated andesite (the South Oromocto Andesite); an alluvial fan deposit, which grades from pebble- to cobble-conglomerate at the bottom to mudstone with intercalated calcrete at the top. An unwelded pumiceous lapilli tuff occurs in the lower part of the section and a basalt flow occurs in the upper part (the Carrow Formation); and a quartz- and feldspar-phyric lava flow that is characterized by large K-feldspar (≤20%), quartz, and plagioclase phenocrysts with accessory minerals of apatite, zircon, and titanomagnetite (The Bailey Rock Rhyolite) (Fig. 1).

The intracaldera sequence, in ascending stratigraphic order, consists of greenish-grey sedimentary breccia and interbedded andesitic lava flows, but locally dominated by felsic pyroclastic rocks (The Scoullar

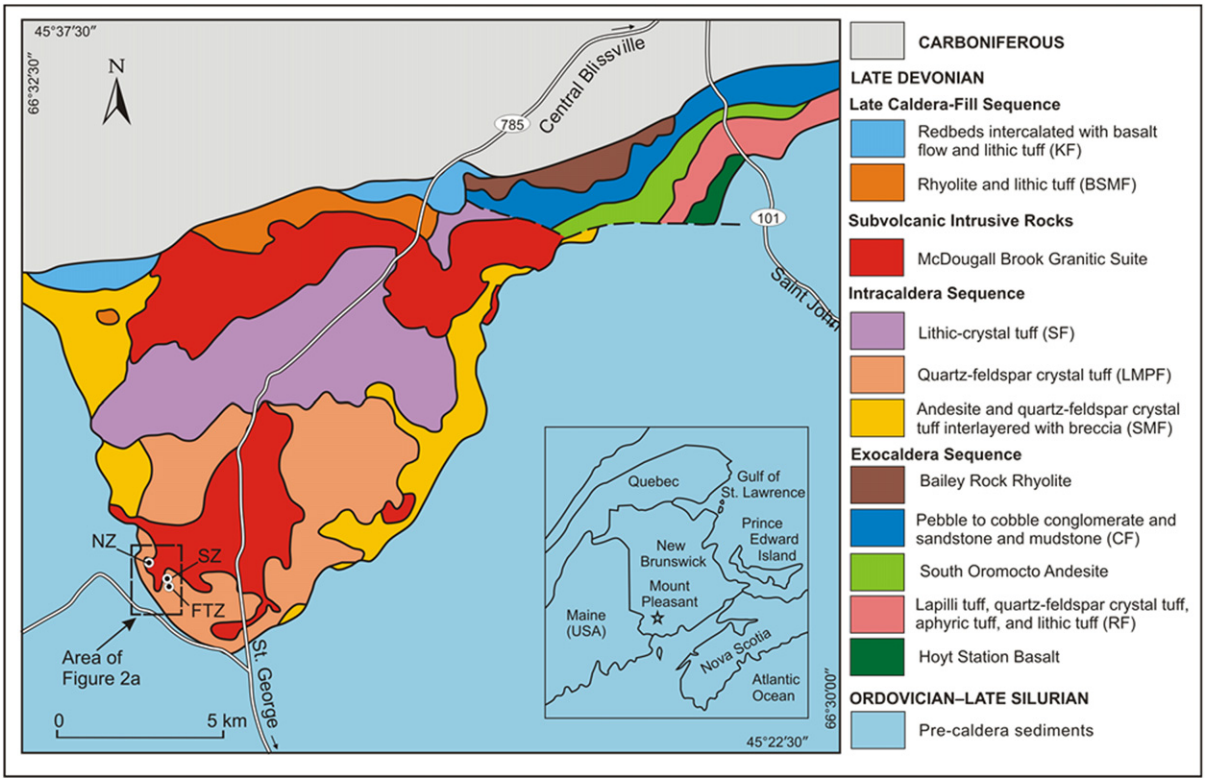

Fig. 1. Geology of the Mount Pleasant Caldera Complex (modified from McCutcheon et al., 2010) showing location of mineralized zones at the Mount Pleasant mine site. RF-Rothea Formation, CF-Carrow Formation, SMF-Scoullar Mountain Formation, LMPF-Little Mount Pleasant Formation, SF-Seelys Formation, BSMF-Big Scott Mountain Formation, KF-Kleef Formation, NZ-North Zone, SZ-Saddle Zone, FTZ-Fire Tower Zone.

Mountain Formation); pumiceous quartz-feldspar crystal tuff (The Little Mount Pleasant Formation); densely welded, pumiceous, lithic-crystal tuff (The Seelys Formation); and the McDougall Brook Granitic Suite (Fig. 1).

The late caldera-fill sequence comprises the Big Scott Mountain and Kleef formations in ascending order. The Big Scott Mountain Formation has three units from bottom to top that consist of porphyritic to nearly aphyric rhyolite, lithic to lithic-lapilli tuff, and crystal tuff. The Kleef Formation, from base to top, includes conglomeratic redbeds, porphyritic to glomeroporphyritic basalt and pumiceous, lithic tuff to lithic lapilli tuff. (McCutcheon, 1990; McCutcheon et al., 1997) (Fig. 1). Nonetheless it has proven very difficult to identify these felsic volcanic units in the field, because of their lack of distinctive textural characteristics (Thorne et al., 2013).

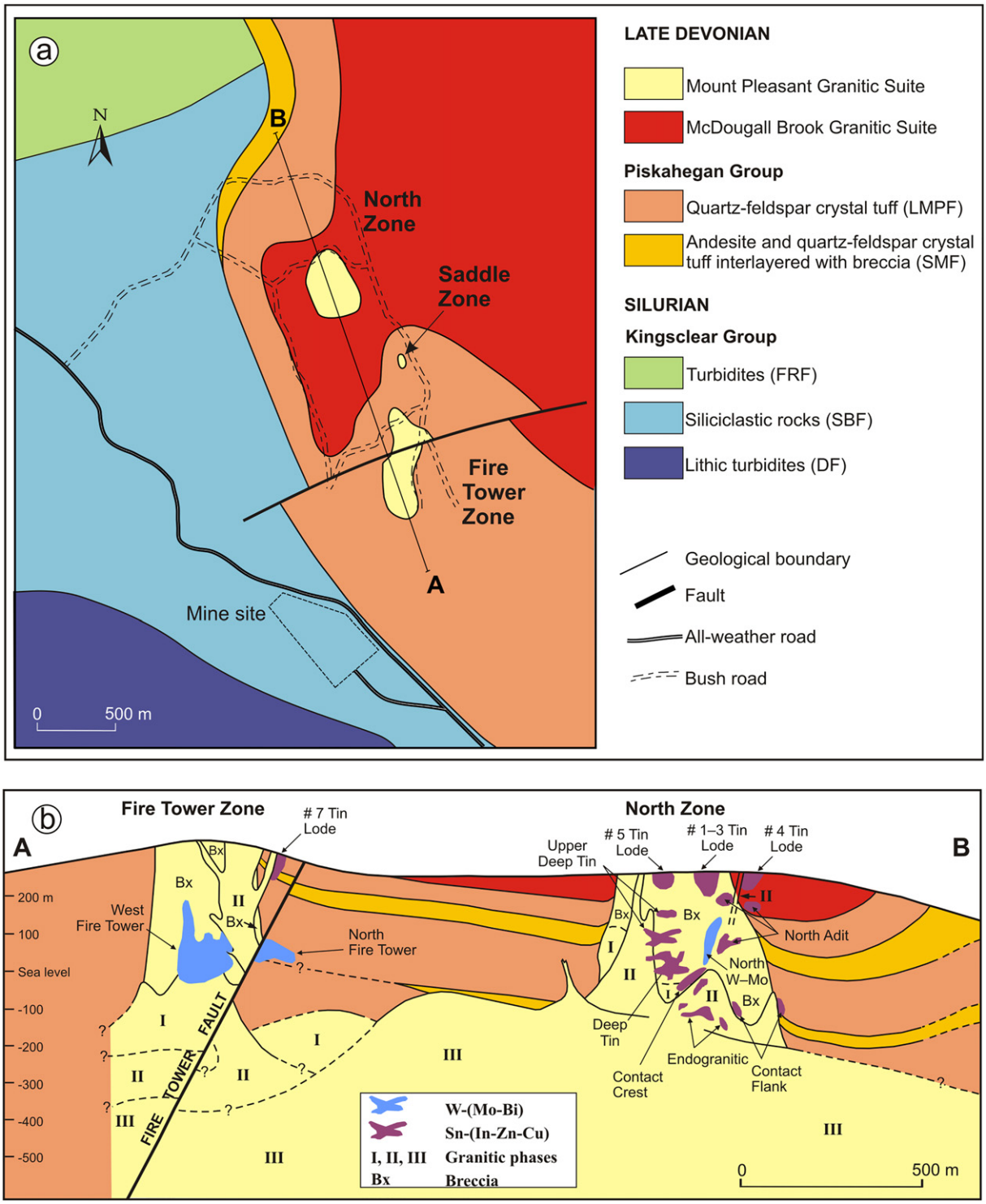

Fig. 2. (a) Detailed geology map of the Mount Pleasant deposit showing the location of the Fire Tower Zone (FTZ), North Zone (NZ), and cross-section A-B (modified after McCutcheon et al., 2010). (b) Cross-section of Mount Pleasant deposit looking southwest (modified after Dunbar et al., 2008; McCutcheon et al., 2012). DF-Digdeguash Formation, SBF-Sand Brook Formation, FRF-Flume Ridge Formation, SMF-Scoullar Mountain Formation, LMPF-Little Mount Pleasant Formation.

The country rocks of the Fire Tower Zone and the North Zone of the Mount Pleasant polymetallic deposits include the Scoullar Mountain Formation and the Little Mount Pleasant Formation (Fig. 2). Overlying a rhyodacitic flow of feldspar porphyry is likely an extrusive equivalent of the McDougall Brook Granitic Suite (MBGS, McCutcheon, 1990; McCutcheon et al., 1997). The 2008 NI 43-101 compliant resource report for the Fire Tower Zone states an indicated total resource of 13.48 Mt. grading 0.33% WO_3, 0.21% MoS_2, and 0.06% Bi with an inferred resource of 841,700 t at 0.26% WO_3, 0.20% MoS_2, and 0.04% Bi (Dunbar et al., 2008). For the North Zone, the 2012 NI 43-101 compliant resource report states an indicated resource of 12.4 Mt. grading 0.38% Sn, 0.86% Zn, and 64 ppm In, and an inferred resource of 2.8 Mt. grading 0.30% Sn, 1.13% Zn, and 70 ppm In (McCutcheon et al., 2012). Alteration in the Mount Pleasant deposit includes intense and pervasive greisen-type alteration consisting of quartz-topaz-sericite-fluorite alteration associated mainly with the orebodies and quartz-biotite-chlorite-topaz alteration associated with lower grade zones. Propylitic alteration (chlorite + sericite) extends for hundreds of metres beyond the mineralized zones. Potassic alteration occurs locally, mainly in Granite I (Kooiman et al., 1986).

The ages of the MPGS and associated mineralizing systems have been inferred by dating of various rock units in this area. Sinclair and Kooiman (1990) reported radiometric dates for GIII using $^{40}Ar/^{39}Ar$ ages obtained from biotite in sedimentary breccia underlain by granite dated at ca. 361 Ma. The Bailey Rock Rhyolite has a U-Pb zircon age of 363.4 ± 1.8 Ma (Tucker et al., 1998) and the Piskahegan Group has a Rb-Sr age of 368 Ma (Anderson, 1992). Thorne et al. (2013) reported Re-Os ages of 369.7 ± 1.6 Ma and 370.1 ± 1.7 Ma from samples of molybdenite related to the Granite I intrusive phase and the W-Mo mineralization from the Fire Tower Zone. These ages confirm that caldera formation, volcanism, and subvolcanic intrusions were formed during a relatively short time (Yang et al., 2003).

3. Methodology

Fifty-four samples in the Fire Tower Zone and sixty-three samples in the North Zone were collected from surface exposures. All of the samples were photographed and their locations were recorded using a GPS in the field (Figs. 3, 4). The samples were cut and dried in the lab of New Brunswick Department of Energy and Mines in order to obtain a flat surface (ca. 40–100 cm^2) to facilitate the pXRF analysis.

Six regularly spaced spots on flat surface of each sample were measured by the Olympus X-5000 pXRF spectrometer using 'soil mode' with three beams. In order to avoid mixed compositions of the breccia, six analysis spots were chosen on fragments of the felsic breccia samples and on matrix of the chloritic breccia samples. Beam 1 (50 kV, 120 s) measures U, Sr, Zr, Th, Mo, Ag, Cd, Sn, Sb, and Ba. Beam 2 (35 kV, 40 s) measures Fe, Co, Ni, Cu, Zn, Hg, As, Se, Pb, Bi, and Rb. Beam 3 (15 kV, 120 s) measures P, S, Cl, K, Ca, Ti, Cr, and Mn. Calibration checks were done twice per day. A quartz blank and seven certified reference materials (CRMs) were analysed during the measurement process, in order to monitor the instrumental drift and obtain the correction factors for each element, respectively. These CRMs include two samples from the National Institute of Standards and Technology (NIST) SRM2702 (inorganics in marine sediment) and SRM2781 (domestic sludge); and five samples from the Canadian Certified Reference Materials Project (CCRMP) SY-2 (syenite), SY-4 (diorite gneiss), Till-3 (till), MP-1 (a zinc-tin-copper-lead ore), and DS-1 (a gold ore). Using the repeated analysis of these CRMs, correction factor and precision of each element were calculated. These correction factors were then applied to the raw pXRF data of the samples from the two mineralization zones of the Mount Pleasant (Appendices A and B).

4. Results and discussion

4.1. Data processing

4.1.1. Precision of pXRF data

The precision is defined by the reproducibility of multiple analyses on the same sample and calculated as being twice the relative standard deviation (Thompson and Howarth, 1973; Piercey, 2014). Most commonly, the instrumental precision was simply represented by relative standard deviation (RSD), which is the standard deviation divided by the mean for each element (Stdv/Mean × 100%). For the seven CRMs, the precision for elements Ti, Fe, Mn, Ca, K, V, Ba, and Y is <5%. A few elements have precision values close to 10% including P, Cl, Rb, Sr, Zr, Nb, Cr, Co, Zn, and Pb. Ni, Cu, Mo, Bi, Cd, Sb, Th, As, and Ce have the precision values < 20%. Other elements including S, Se, Ag, Sn, La, W, Hg, and U have poor precision (>20%) values. These poorer results are caused by lower element content in these CRMs. For example, the precision of Sn is <10% when its content is higher than 30 ppm. Tungsten content in most of the standards is below limits of detection and its precision value around 20% at 30 ppm decreases to 7% at 100 ppm (Appendix A).

4.1.2. Calibration of pXRF data

The accuracy of the pXRF data is constrained by the calibration. Plotting of certificated values against measured values of each element in the CRMs, linear regression equations for these elements can be calculated (Appendix A). The r-squared (r^2) is the square of the correlation coefficient indicating the strength of linear association (goodness of fit). The pXRF values have perfect linear association with the certificated values for elements in the CRMs if r^2 value is close to 1. Low concentration elements in the CRMs (i.e., W) are below the limits of detection and thus cannot be calibrated by linear regression. Detailed slope, intercept value, and r^2 for each element are listed in Appendix A. Only Ba and Co have the r^2 values of 0.68 and 0.55, respectively. The rest of analysed elements listed in Table 1 have very strong linear associations with r^2 higher than 0.85. Corrected pXRF data of all samples are shown in Appendix B and summarized in Table 1.

4.2. Lithological units discrimination

The rocks in the Fire Tower Zone and the North Zone are highly altered by hydrothermal fluids (Fig. 4a), thus only immobile elements were selected for rock discrimination. The immobile elements include Al, Ga, Ti, Sc, Zr, Hf, Y, Th, heavy rare-earth elements (HREE), and possibly Nb and Ta (see MacLean and Barrett, 1993; Leitch and Lentz, 1994; Christiansen and Keith, 1996; Jenner, 1996; Kerrich and Wyman, 1996; Lentz, 1996a, 1996b), mass gains and losses of mobile components during the alteration cause the compositional variation of these immobile elements, but their ratios stay the same (MacLean and Barrett, 1993). Immobile compatible-incompatible element pairs are useful tools to monitor the fractionation trends of magmas (MacLean and Barrett, 1993; Barrett and MacLean, 1994). Hall et al. (2014) conducted testing using the Olympus X-5000 pXRF spectrometer to measure those immobile elements of most interest and concluded that only Ti, Nb, and Y can be 'very well' determined, Zr can be 'well' determined, and Th can be 'moderately well' determined. Meanwhile, according to the classification criteria of pXRF data quality introduced by United States Environmental Protection Agency (2007), the pXRF data of elements Ti, Zr, Nb, and Y of this study are "definitive" (r^2 = 0.85–1, RSD ≤ 10%), whereas Th is "quantitative" (r^2 = 0.70–1, RSD ≤ 20%). Thus, Ti, Zr, Nb, Y, and Th are used in this study to discriminate the rock units in the Fire Tower Zone and the North Zone.

The primary subdivision of samples is based on original interpretation of geological map (Fig. 1). However, the later pXRF analysis indicates that the rock units are not classified properly and the geological map in the Fire Tower Zone and the North Zone area needs to be

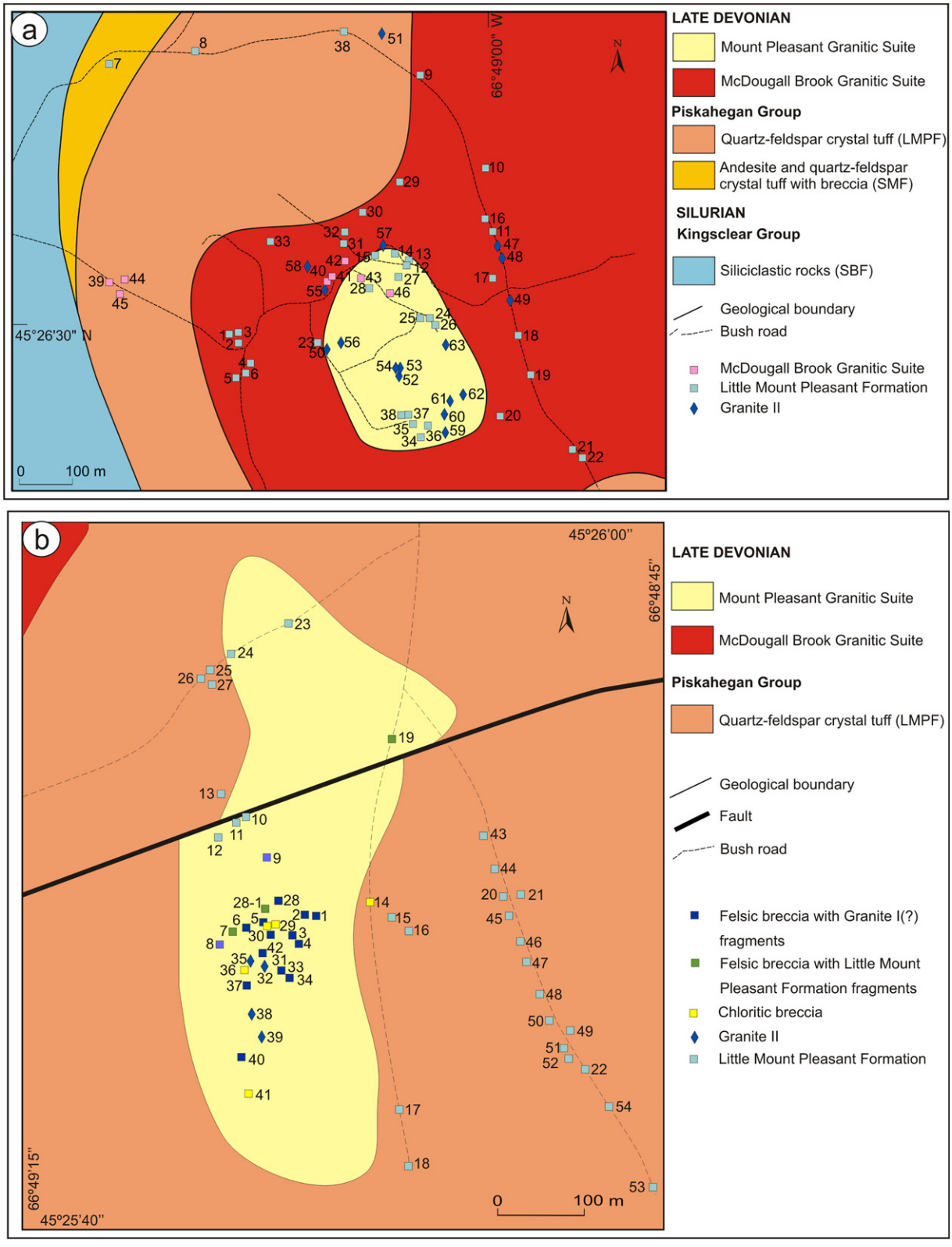

Fig. 3. Local geologic map the North Zone (a) and the Fire Tower Zone (b) showing the locations of hand samples with corresponding rock type discerned from geochemical analysis associated with this study. Numbers are sample numbers in Appendix B. SBF-Sand Brook Formation, SMF-Scoullar Mountain Formation, LMPF-Little Mount Pleasant Formation.

modified (Fig. 3). For example, the sample NZ47 from the McDougall Brook Granitic Suite in the map (Fig. 4b) Appendix B) has immobile elements composition similar as these of Granite II (Fig. 4c). The pink colour of NZ47 is related to surface weathering of the outcrop and the fresh surface is dark grey. The colour and the mineral assemblage of the NZ47 shows it is Granite II and distinct from McDougall Brook Granitic Suite (Figs. 1, 4d). Thus, in this study, the discrimination of the rock units from the Fire Tower Zone and the North Zone were based on the interpretation of the pXRF data and the field observation. The immobile element composition of each unit is briefly described here.

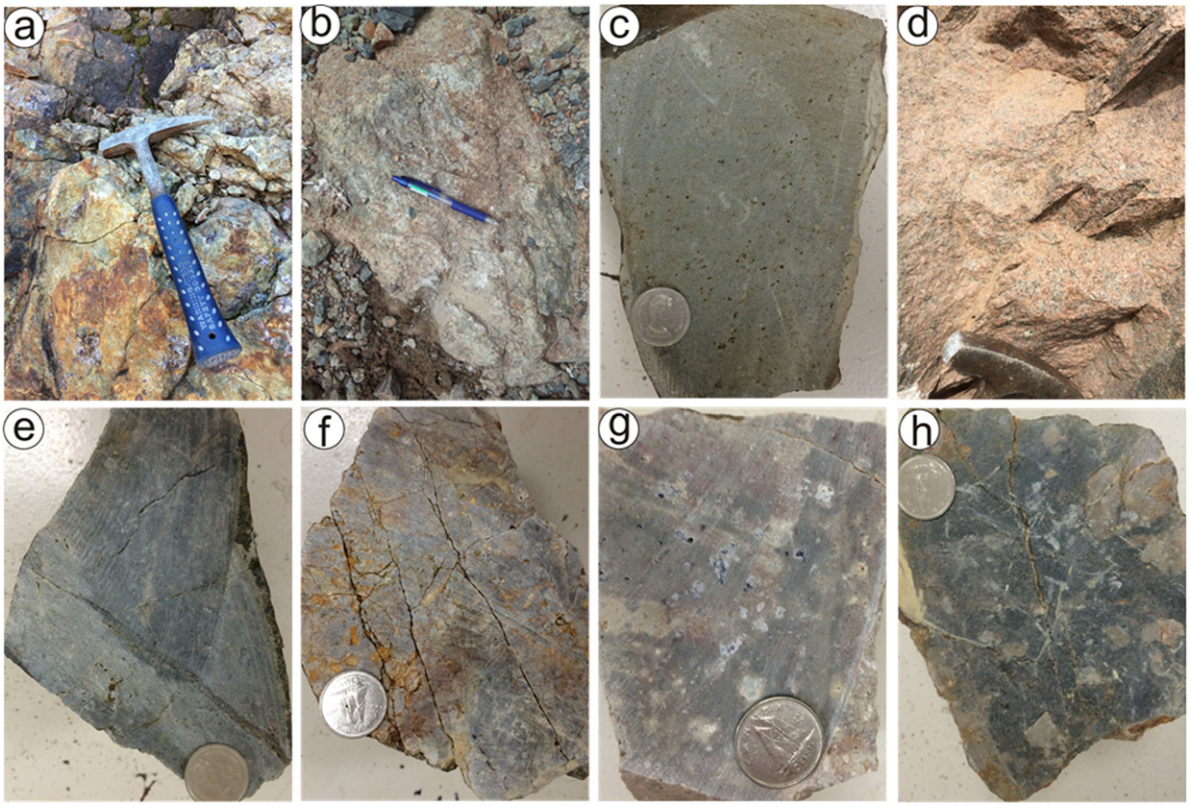

Fig. 4. Representative photos of the rock units from the North Zone and the Fire Tower Zone. (a) strongly altered Little Mount Pleasant Formation with fluorite, (b) interpreted as granite II, (c) granite II, (d) McDougall Brook Granite, (e) Little Mount Pleasant Formation, (f) Little Mount Pleasant Formation fragments in breccia, (g) Granite I fragments in breccia, (h) chlorite breccia.

The analytical results show the unaltered Little Mount Pleasant Formation (Fig. 4e) is characterized by its highest Ti contents (1166–6599 ppm) among the rock units analysed, that is consistent with the reported Ti value of >1000 ppm by Kooiman et al. (1986). The altered Little Mount Pleasant Formation samples identified by this study occur in the mineralization zones. Compared with fresh samples, they have similar immobile element contents but much lower mobile elements (i.e. K). Both fresh and altered samples have the lowest Zr/Ti (<0.1), Nb/Ti (<0.02), Y/Ti (<0.05), and Th/Ti (<0.01) ratios compared to other rock units (Table 1, Figs. 5, 6).

The least-altered granite porphyry (Granite II, Fig. 4c) contains 2% to 5% quartz phenocrysts (1–3 mm in diameter) and 5% to 10% pink K-feldspar phenocrysts (1–5 mm long). Other phenocrysts include 2% to 5% chloritized biotite and 2% to 10% plagioclase. The matrix is light green to pink and fine-grained (0.05–0.1 mm) and consists of a mosaic of quartz and K-feldspar with abundant micrographic textures (Kooiman et al., 1986). The Granite II has 345 to 539 ppm Ti, 79 to 115 ppm Zr, 18 to 81 ppm Nb, 41 to 240 ppm Y, and 10 to 36 ppm Th. The element ratios show they have Zr/Ti of 0.16 to 0.28, Nb/Ti of 0.05 to 0.18, Y/Ti of 0.09 to 0.66, and Th/Ti of 0.02 to 0.08 (Table 1, Figs. 5, 6).

The McDougall Brook Granitic Suite (Fig. 4d), only found in the North Zone, has intermediate immobile element contents, which overlap those of the Little Mount Pleasant Formation and GII to some degree. However, the immobile element ratios effectively subdivides these three groups in the North Zone and all the element ratios increase from the Little Mount Pleasant Formation, through the McDougall Brook Granitic Suite, and to the GII (Table 1, Figs. 5 and 6).

The fragments in the breccia are angular to subrounded, in places tabular, and typically range from 1 to 10 cm in diameter. The original lithologies of the fragments are mostly unknown as alteration has largely destroyed the texture of the original rock and, in extreme cases, has obscured even the outline of the individual fragments (Kooiman et al., 1986). Two types of fragments were identified based on the pXRF data: 1) the Little Mount Pleasant Formation fragments (Fig. 4f) those have lower Ti content ranging from 858 to 1135 ppm, but has similar Zr/Ti, Nb/Ti, Y/Ti, and Th/Ti ratios than the composition of Little Mount Pleasant Formation; and 2) the white to buff-coloured felsic breccia (Fig. 4g) with greisenized fragments that have the lowest Ti (<430 ppm). The Zr/Ti (0.25 to 0.33), Nb/Ti (0.14 to 0.22), Y/Ti (0.11 to 0.47), and Th/Ti (0.03 to 0.09) ratios of the fragments in the felsic breccia partially overlap with, but are slightly higher than those of Granite II. Considering the hosting breccia is directly in contact with Granite I and cut by GII, these fragments are most likely from Granite I (Table 1, Figs. 5, 6).

The chloritic breccia (Fig. 4h) consists of greisenized fragments in a chloritic matrix that forms 20% to 50% of the rock. The groundmass of the chloritic breccia is fine grained (0.05–0.1 mm) and therefore it is possible to measure the composition by pXRF. Five samples have 441 to 544 ppm Ti, 85 to 193 ppm Y, 100 to 116 ppm Zr, and 27 to 34 ppm Th. However, their trace element ratios overlap with Granite II (Table 1, Figs. 5, 6) and are also close to the reported values of Granite I (Taylor et al., 1985; Kooiman et al., 1986). Kooiman et al. (1986) suggested the chloritic breccia is related to the emplacement of Granite II. Sharp contact relationships indicate that chloritic breccia is younger than the felsic breccia (Kooiman et al., 1986). Due to the similarity of immobile element compositions between Granite I and II as reported by Taylor et al. (1985), Kooiman et al. (1986), Yang et al. (2003), and Inverno and Hutchinson (2006), it is difficult to classify these rocks, if only based on the geochemical data. Field contact relationships show these chloritic breccias were spatially associated with Granite II and, in

Table 1
Summary of statistical values for the corrected pXRF data of samples from the Fire Tower Zone and the North Zone. Detailed data is in Appendix B.

Elements	Units	Granite I fragments in breccia		Matrix of chloritic breccia		LMPF* fragments in breccia		LMPF*		MGBS*		Granitic II	
		n=13		n=5		n=3		n=67		n=8		n=21	
		Ave.*	Sd.*	Ave.	Sd.	Ave.	Sd.	Ave.	Sd.	Ave.	Sd.	Ave.	Sd.
Ti	ppm	376	+26 –24	478	+43 –40	982	+148 –128	2155	+ 1029 –697	962	+442 –303	422	+51 –46
Fe	wt.%	1.13	+0.43 –0.31	2.64	+2.43 –1.27	0.98	+0.08 –0.07	4.67	+3.8 –2.09	1.88	+1.64 –0.88	2.63	+2.56 –1.3
Mn	ppm	8	+104 –8	143	+2351 –136	0	+0 –0	764	+1696 –527	19	+312 –19	119	+2937 –115
Ca	wt.%	0.79	+11.89 –0.74	1.16	+0.85 –0.49	0.08	+24.05 –0.08	0.71	+4.4 –0.61	1.11	+1.45 –0.63	0.09	+7.46 –0.09
K	wt.%	0	+0.17 –24	0.04	+9.71 –0.04	0	+0 –0	0.72	+20.88 –0.70	0	+1.06 –0	0.03	+3.92 –0.03
S	ppm	599	+3776 –517	1005	+ 1056 –515	1594	+3056 –1048	730	+2589 –570	750	+16426 –718	1314	+2192 –822
Rb	ppm	8	+63 –8	28	+626 –28	0	+0 –0	155	+755 –129	16	+148 –15	58	+558 –54
Ba	ppm	0	+0 –0	1	+9 –2	0	+0 –0	46	+500 –43	3	+18 –3	0	+3 –1
Sr	ppm	0	+1 –1	2	+1 –1	0	+0 –0	3	+14 –3	3	+15 –3	1	+2 –1
Nb	ppm	63	+12 –10	64	+19 –15	21	+12 –8	14	+4 –3	18	+18 –9	51	+23 –16
Zr	ppm	110	+9 –9	109	+6 –6	127	+16 –14	176	+72 –51	134	+60 –41	97	+11 –10
Y	ppm	86	+51 –32	129	+53 –37	54	+19 –14	35	+17 –11	59	+ 88 –36	103	+75 –44
Th	ppm	24	+13 –8	29	+3 –3	11	+9 –5	6	+3 –2	10	+8 –5	21	+8 –6
U	ppm	11	+9 –5	11	+9 –5	7	+2 –2	2	+4 –2	3	+7 –2	11	+6 –4
Ce	ppm	16	+154 –15	78	+30 –22	98	+68 –40	142	+47 –35	122	+28 –23	62	+190 –47
Cr	ppm	1	+3 –1	4	+17 –4	1	+3 –1	23	+23 –12	9	+22 –7	5	+10 –4
V	ppm	0	+0 –0	1	+5 –1	0	+0 –0	16	+71 –14	1	+3 –1	0	+0 –0
Cu	ppm	47	+151 –36	66	+473 –59	61	+140 –43	37	+83 –26	19	+199 –18	33	+42 –19
Zn	ppm	129	+321 –92	2 44	+854 –190	318	+3505 –293	253	+298 –137	151	+1456 –138	343	+1274 –271
Sn	ppm	33	+115 –26	90	+627 –79	37	+78 –26	36	+46 –20	24	+245 –23	51	+122 –36
Mo	ppm	37	+79 –26	33	+105 –26	149	+272 –97	17	+49 –13	29	+321 –27	20	+104 –18
As	ppm	298	+796 –217	287	+2780 –261	896	+788 –420	68	+225 –53	270	+6820 –261	115	+877 –103

*LMPF Little Mount Pleasant Formation; MBGS Mcdougall Brook Granitic Suite; Ave, geomatic mean; Sd, standard deviation

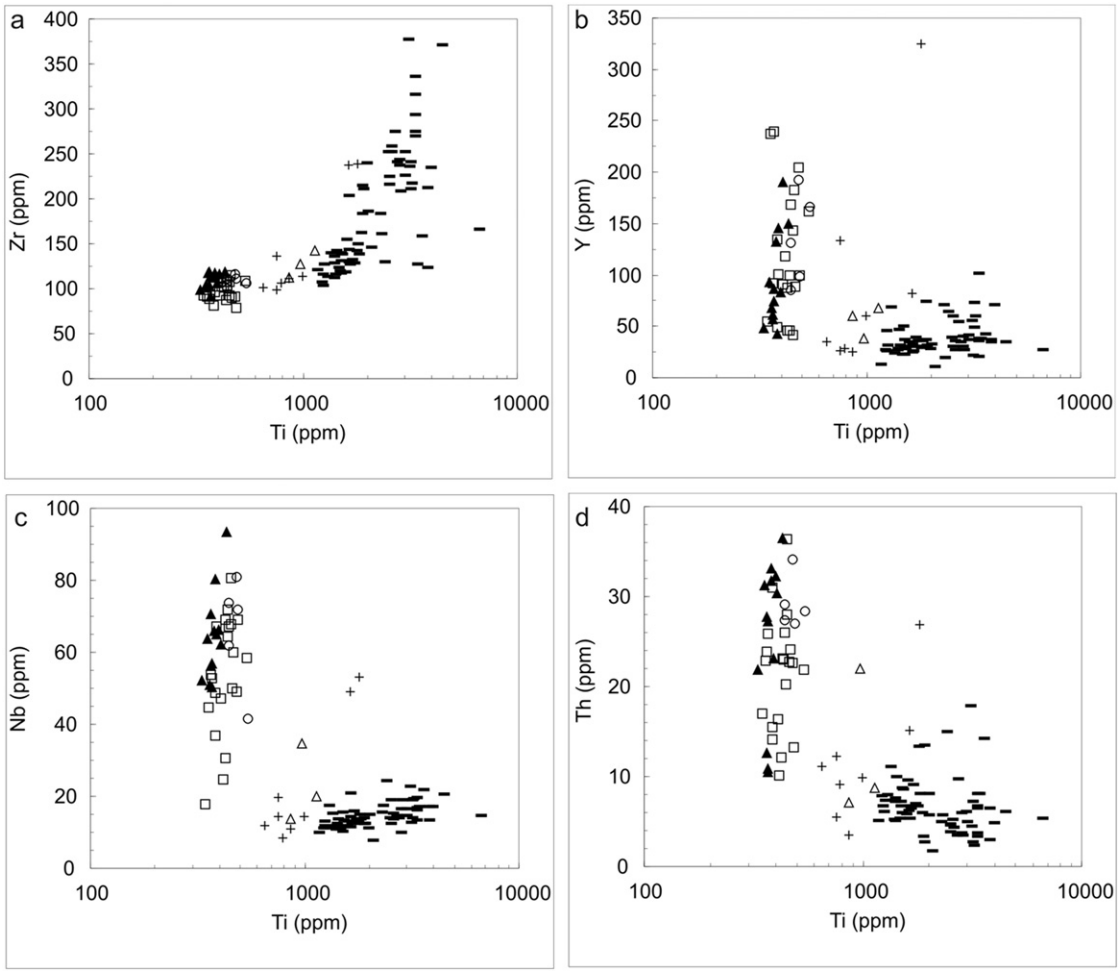

Fig. 5. Immobile element discrimination diagrams of (a) Zr vs. Ti, (b) Y vs. Ti, (c) Nb vs. Ti, and (d) Th vs. Ti pXRF data showing the geochemical variation of the Fire Tower Zone and the North Zone samples. - Little Mount Pleasant Formation, Δ Felsic breccia with Little Mount Pleasant Formation fragments, □ Granite II (GII), ▲ felsic breccia with Granite I fragments, ○ chloritic breccia, + McDougall Brook Granitic Suite.

places, occur at or near their contacts (Kooiman et al., 1986). Thus, the chloritic groundmass is probably from altered Granite I or is Granite II tuffisite.

4.3. Indicator of alteration

Kooiman et al. (1986) suggested that greisen-type alteration is the main alteration type and appears to grade outward into propylitic alteration. Potassic alteration occurs locally. The greisen-type alteration has two assemblages including intense and pervasive quartz-topaz-sericite-fluorite alteration associated mainly with the orebodies and grades laterally into quartz-biotite-chlorite-topaz alteration associated with lower grade zones. The propylitic-type alteration consists mainly of chlorite and sericite. Although pXRF technology does not have the same accuracy or precision as conventional XRF, it may still be useful to show element variations during alteration. Here only using the Pearce et al. (1984) Nb-Y and Rb-Nb + Y diagrams as reference to show the element variation during alteration. The immobile elements Nb and Y of all rock units in both the Fire Tower Zone and the North Zone are slightly or not affected by later hydrothermal alterations. Thus, in the Nb-Y diagram (Fig. 7a), all these units plot in the positions similar as fresh samples reported by previous studies (Kooiman et al., 1986; Yang et al., 2003; Inverno and Hutchinson, 2006). However, in the Rb-Nb + Y diagram (Fig. 7b), since the Rb behaves in the same way as K due to their similarities in size, charge, and electronegativity, and during the later greisen-type and chloritization alteration processes in the Mount Pleasant area, the K and Rb were leached out. Thus, in the Fire Tower Zone, the GI fragments in breccia and GII have obvious Rb depletion and some samples of them plot close to the bottom of the Rb-Nb + Y diagram. The fragments of the Little Mount Pleasant Formation in the breccia have the Rb content lower than the limits of detection (Table 1). In the North Zone, the similar Rb depletion was found in the GII and the McDougall Brook Granitic Suite. Most samples of the Little Mount Pleasant Formation are far away from the mineralization zone and thus were less or unaltered.

4.4. Indicator of mineralization

Principal components analysis (PCA) is a useful multivariate statistical technique for identifying complex associations, which has been used by geologists to study geochemical anomalies associated with various hydrothermal alteration and mineralization types (Grunsky, 1986, 2010; Shikazono et al., 2008; Zuo, 2011; Wang et al., 2013; Wang et al., 2014; Shahi et al., 2015), metal pollution in sediments (Rubio et al., 2000), and petrology (Ragland et al., 1997). The objective of PCA is to reduce the dimensionality of a large dataset by transforming interrelated variables into new uncorrelated artificial variables (principal components) in decreasing order (Jolliffe, 2002). PCA was performed on the pXRF dataset for both the Fire Tower Zone and the North Zone by correlation matrix analysis. The extracted principal components (PCs) were subjected to orthogonal rotation by the Varimax method to maximize

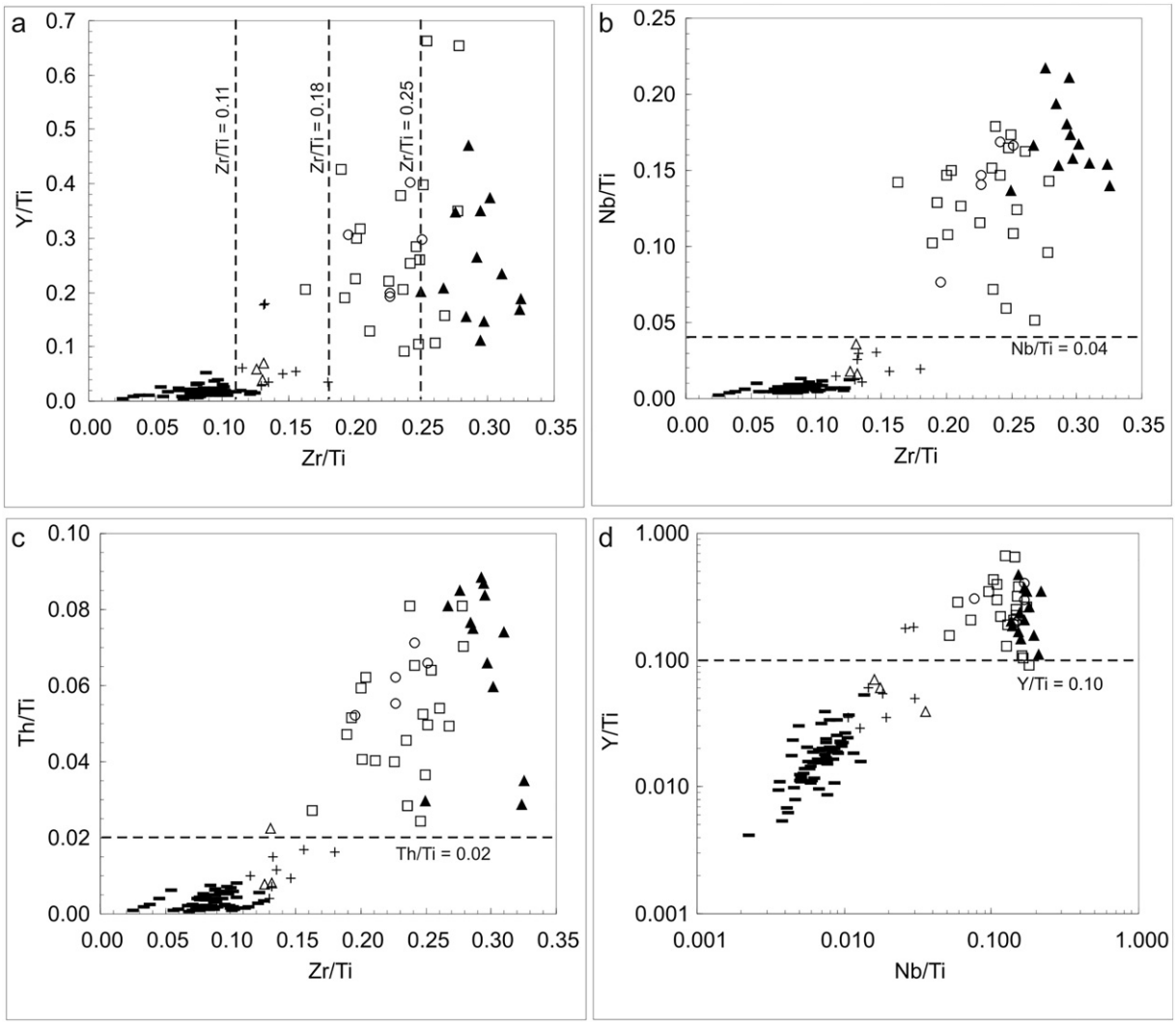

Fig. 6. Immobile element discrimination diagrams of (a) Y/Ti vs. Zr/Ti, (b) Nb/Ti vs. Zr/Ti, (c) Th/Ti vs. Zr/Ti, and (d) Y/Ti vs. Nb/Ti pXRF data for all samples from the Fire Tower Zone and the North Zone. See Fig. 5 for symbols.

the variability among all input variables, and thus facilitate interpretation of the factor loadings (Kaiser, 1960).

For the whole pXRF data of the Fire Tower Zone and the North Zone, six PCs with eigenvalues larger than 1 and in this study (Fig. 8a), the first three of them have geological meaning and were chosen for further discussion. These first three PCs explaining c. 60% of the total variance (Table 2), likely reflect the main rock types and mineralization processes in the Mount Pleasant area (Fig. 8b, c, and d). The PC1 represents 35% of the total variance (Table 2) and have positive loadings of Ti, Zr, Ce, Cr, and V and the negative loadings of Nb, Y, U, and Th. Since these elements

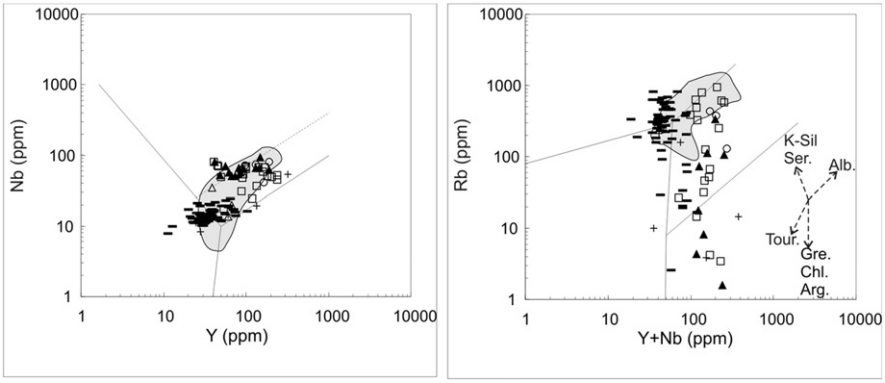

Fig. 7. Possible alteration effects on Rb, Nb, and Y compositions measured by pXRF for the samples of the Fire Tower Zone and North Zone. Diagrams were modified from Pearce et al. (1984). Grey area is the published data for the Little Mount Pleasant, the Mount Pleasant Granitic Suites, and the McDougall Brook Granitic Suites (Kooiman et al., 1986; Yang et al., 2003; Inverno and Hutchinson, 2006). Alteration types listed here are K-silicate (K-sil.), sericitic (Ser.), argillic (Arg.), chloritization (Chl.), tourmalinization (Tour.), greisen (Gre.), and albitization (Alb.). See Fig. 5 for symbols.

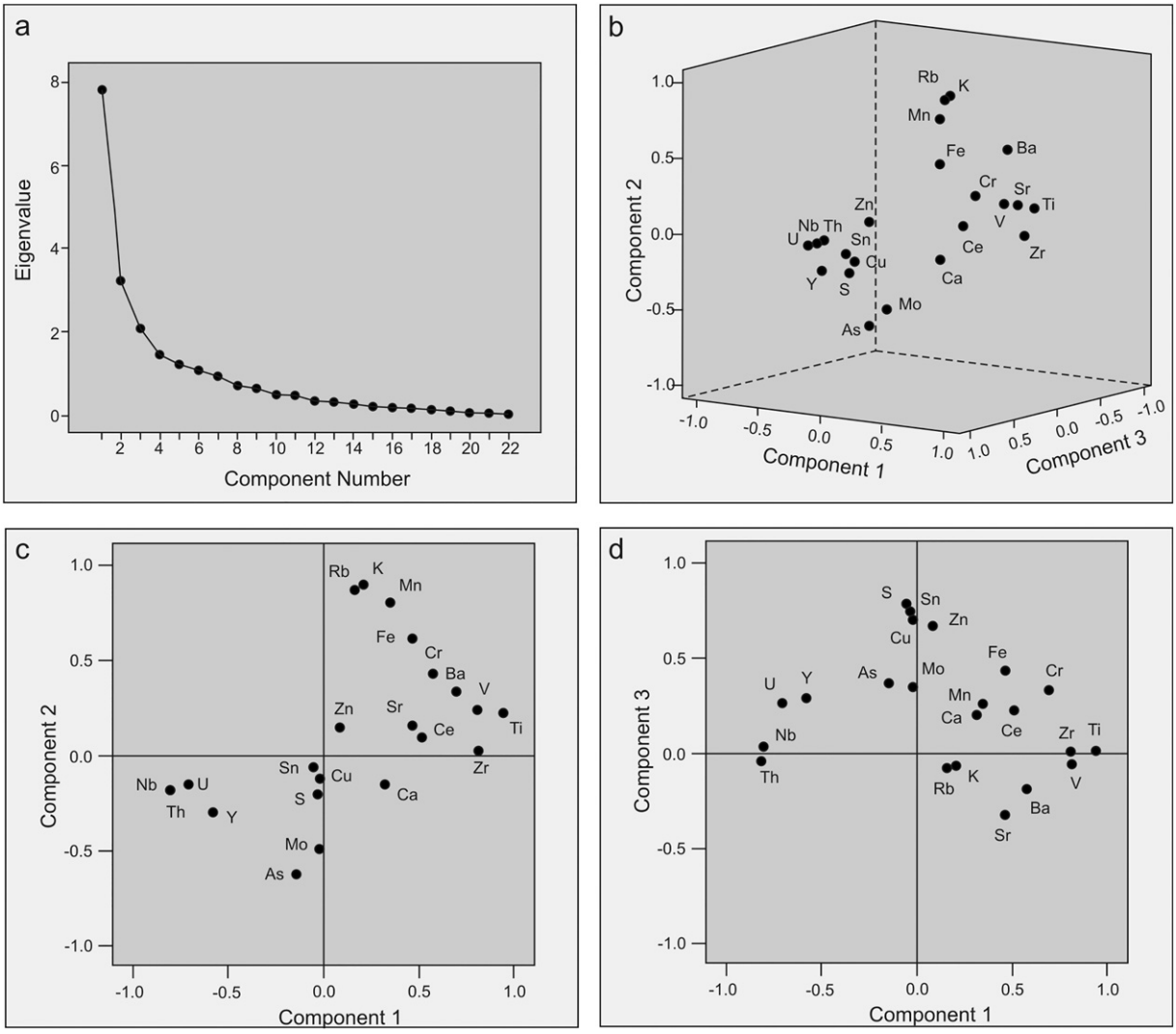

Fig. 8. (a) Scree plot of eigenvalues of principal components (PC1-PC22), (b) 3D plots, and (c and d) biplots of rotated principal components of pXRF data in rotated space for pXRF data of all samples from the Fire Tower Zone and the North Zone.

are mainly rock forming elements and are generally considered as immobile elements during later hydrothermal activities, the PC1 are interpreted to represent the geochemical variations of the lithologic units in this area (Figs. 8b and c, Table 3). The PC2, explaining 15% of the total variance (Table 2), is characterized by high-positive loadings for K, Rb, Fe, and Mn and negative loadings of As and Mo (Fig. 8b and c, Table 3). The PC2 is interpreted to represent the W-Mo mineralization in the Mount Pleasant area. The high-grade W-Mo orebodies are mainly associated with pervasive quartz-topaz-sericite-fluorite alteration which shows strong depletion in Fe, Mn, K, and Rb as indicated by Pouliot et al. (1978) and Kooiman et al. (1986). Consequently, samples with lower PC2 factor scores have more chance of containing high-grade Mo contents. The PC3 accounts for c. 9% of the total variance (Table 2). The positive loadings of Sn, Zn, Cu, and S and slightly negative loadings of Sr and Ba indicate that the PC3 is associated with the Sn-Zn mineralization (Fig. 8b and d, Table 3). Thus the PC3 factor score could be used as the Sn mineralization indicator in the Mount Pleasant area.

4.5. Potential impact on exploration strategies

This study has shown that the pXRF analysis has the potential to improve the understanding of stratigraphy and mineralization in the Mount Pleasant deposit area. The pXRF analysis gives geologists greater confidence in models than would have been possible without these data (Gazley et al., 2015). A comprehensive model for the evolution of the Mount Pleasant Caldera Complex was presented by McCutcheon (1990) based on the concept of a single caldera cycle. However, new geochronological data indicated that this model needs to be modified (Thorne et al., 2013). The pXRF can be used here to investigate the spatial distribution of geochemical elements of the Mount Pleasant Caldera

Table 2
Total variance explained in PCA method for pXRF data of samples from the Fire Tower Zone and the North Zone.

Component	Initial eigenvalues			Extraction sums of squared loadings			Rotation sums of squared loadings		
	Total	% of variance	Cumulative %	Total	% of variance	Cumulative %	Total	% of variance	Cumulative %
1	7.808	35.490	35.490	7.808	35.490	35.490	6.111	27.777	27.777
2	3.231	14.685	50.176	3.231	14.685	50.176	3.903	17.740	45.517
3	2.090	9.499	59.674	2.090	9.499	59.674	3.115	14.157	59.674

Table 3
Component matrix and Varimax rotated component matrix for pXRF data of samples from the Fire Tower Zone and the North Zone. Values in bold are the most positive or negative values of that principal component.

	Component Matrix			Rotated Component Matrix		
	1	2	3	1	2	3
Ti	0.890	0.193	–0.287	**0.931**	0.214	0.011
Fe	0.639	0.378	0.343	0.457	**0.528**	0.426
Mn	0.700	0.128	0.551	0.341	**0.791**	0.261
Ca	0.153	0.307	–0.210	0.309	–0.161	0.201
K	0.656	–0.238	0.580	0.198	**0.883**	–0.067
S	–0.210	0.742	0.117	–0.044	–0.213	**0.749**
Rb	0.610	–0.252	0.574	0.158	**0.856**	–0.078
Ba	0.790	–0.173	0.083	0.571	**0.546**	**–0.192**
Sr	0.488	–0.222	–0.224	0.460	0.148	**–0.323**
Nb	–0.783	–0.124	0.262	**–0.812**	–0.192	0.036
Zr	0.678	0.146	–0.411	**0.804**	0.011	–0.060
Y	–0.679	0.199	0.142	**–0.584**	–0.313	0.287
Th	–0.779	–0.200	0.242	**–0.817**	–0.186	–0.042
U	–0.702	0.107	0.317	**–0.712**	–0.163	0.265
Ce	0.452	0.315	–0.103	0.507	0.087	0.223
Cr	0.721	0.400	0.033	**0.685**	0.321	0.330
V	0.786	0.156	–0.213	**0.798**	0.224	0.011
Cu	–0.152	0.686	0.159	–0.030	–0.133	**0.707**
Zn	0.087	0.605	0.300	0.077	0.131	**0.664**
Sn	–0.146	0.731	0.240	–0.053	–0.077	**0.777**
Mo	–0.323	0.442	–0.268	–0.023	**–0.505**	0.342
As	–0.503	0.462	–0.295	–0.154	**–0.630**	0.364

Complex and the obtained datasets are then interpreted by PCA. Each principal component with geological meaning could produce a score map to show the distribution of different rock units or mineralization/alteration (e.g. Wang et al., 2014). Systematic pXRF analysis of drill cores of the Mount Pleasant deposit can produce a 3D model to show different rock units or mineralization based on either element concentrations (e.g. Gazley et al., 2011a) or PCA scores (e.g. Chen et al., 2015). These models built on the large pXRF datasets can guild the exploration activities in this area and attribute metallurgical performance to predict metallurgical recovery in different ore blocks (Gazley et al., 2011a).

5. Conclusion

Rock units in the Fire Tower Zone and the North Zone are complicated due to variable intensity of episodic hydrothermal alteration. It is difficult to discriminate the visually similar textures and mineral assemblages in these samples, especially for the breccias. The portable XRF technology, which is able to obtaining large dataset efficiently, offered reliable chemical composition information for identifying different rock units. The raw pXRF data was calibrated by linear regression equations defined by plotting measure values against certificated values of seven certificated reference materials (CRMs). The results of this research include:

1) The immobile elements Ti, Zr, Nb, Y, and Th effectively discriminate felsic rock units in the Fire Tower Zone and the North Zone. The Little Mount Pleasant Formation is characterized by its highest Ti and Zr and the MPGS (GI and GII) has the highest Y, Nb, and Th. The MBGS has the intermediate composition between them. The element ratios of Zr/Ti, Nb/Ti, Y/Ti, and Th/Ti increase from the Little Mount Pleasant Formation, through the McDougall Brook Granitic Suite, and to the MPGS (GI and GII).

2) In comparison with the immobile elements Nb and Y, some rock units (mostly the breccia) have significant Rb and K depletion that was caused by greisen-type alteration close to the orebodies and distal propylitic alteration. The elements Fe and Mn might also be leached out from the mineralization system during the strong greisen alteration process in the breccia.

3) The PCA was used to simplify the whole pXRF datasets. The PC1 for the pXRF data from both zones represents the various rock units in these areas and thus the regression factor scores for each group are different. The PC2 accounts for the W-Mo mineralization in the Mount Pleasant area indicating by the enrichment of Mo and As and depletion of Fe, Mn, K, and Rb associated with greisen alteration in these felsic rocks. The PC3 has the positive loading of Sn-Zn-Cu-S and thus can be used as a Sn-Zn mineralization indicator in this area.

Supplementary data to this article can be found online at http://dx.doi.org/10.1016/j.gexplo.2017.02.005.

Acknowledgements

This research is funded by a NSERC Discovery (217095) grant to Dave Lentz. The New Brunswick Department of Energy and Mines, especially Dr. Kay Thorne, is thanked for use of their portable X-ray fluorescence (pXRF) spectrometer and Adex Mining Inc. is thanked for permitting access to the Mount Pleasant property. Eric Garcelon assisted with field sampling.

References

Anderson, H.E., 1992. A Chemical and Isotopic Study of the Age, Petrogenesis and Magmatic Evolution of the Mount Pleasant Caldera Complex, New Brunswick. (Unpublished Ph.D Thesis). Carleton University, Ottawa, Ontario (203 pp.).
Arne, D.C., Mackie, R.A., Jones, S.A., 2014. The use of property-scale portable X-ray fluorescence data in gold exploration: advantage and limitations. Geochem. Explor. Environ. Anal. 14, 233–244.
Barrett, T.J., MacLean, W.H., 1994. Chemostratigraphy and hydrothermal alteration in exploration for VHMS deposits in greenstones and younger volcanic rocks. In: Lentz, D.R. (Ed.), Alteration and Alteration Processes associated with Ore-forming Systems. Geol. Assoc. Can., Short Course Notes 11, pp. 433–467.
Charnley, B.E., Lentz, D.R., 2015. Petrogeochemical assessment of the various felsic volcanic and subvolcanic igneous rocks associated with Sn-Cu-Zn and W-Mo-Bi mineralization in the North Zone, Mount Pleasant, New Brunswick: a pXRF study. New Brunswick Department of Energy and Mines, Geological Surveys Branch, Geoscience Report 2015-5 (31 pp.).
Chen, S., Grunsky, E.C., Hattori, K., Liu, Y., 2015. Principal component analysis of geochemical data from the REE-rich Maw Zone, Athabasca Basin, Canada. Geol. Surv. Canada Open File 7689, 1–21.
Christiansen, E.H., Keith, J.D., 1996. Trace element systematics in silicic magmas: a metallogenic perspective. In: Wyman, D.A. (Ed.), Trace Element Geochemistry of Volcanic Rocks: Applications for Massive Sulphide Exploration. Geol. Assoc. Can., Short Course Notes 12, pp. 115–152.
Dunbar, P., El-Rassi, D., Rogers, J.A., 2008. A Technical Review of the Mount Pleasant property, Including an Updated Mineral Resource Estimate on the Fire Tower Zone, Southwestern New Brunswick for Adex Mining Inc. Watts, Griffis and McOuat (130 pp.).
Fisher, L., Gazley, M.F., Baensch, A., Barnes, S.J., Cleverley, J., Duclaux, G., 2014. Resolution of geochemical and lithostratigraphic complexity: a workflow for application of portable X-ray fluorescence to mineral exploration. Geochem. Explor. Environ. Anal. 14, 149–159.
Gazley, M.F., Duclaux, G., Fisher, L.A., de Beer, S., Smith, P., Taylor, M., Swanson, R., Hough, R.M., Cleverley, J.S., 2011a. 3D visualization of portable X-ray fluorescence data to improve geological understanding and predict metallurgical performance at Plutonic Gold Mine, Western Australia. Trans. Inst. Min. Metall. Sect. B 120, 88–96.
Gazley, M.F., Vry, J.K., Plessis, E., Handler, M.R., 2011b. Application of portable X-ray fluorescence analyses to metabasalt stratigraphy, Plutonic Gold Mine, Western Australia. J. Geochem. Explor. 110, 74–80.
Gazley, M.F., Duclaux, G., Fisher, L.A., Tutt, C.M., Latham, A.R., Hough, R.M., De Beer, S.J., Taylor, M.D., 2015. A comprehensive approach to understanding ore deposits using portable X-ray fluorescence (pXRF) data at the Plutonic Gold Mine, Western Australia. Geochem. Explor. Environ. Anal. 15, 113–124.
Govett, G.J.S., Atherden, P.R., 1988. Application of rock geochemistry to productive plutons and volcanic sequences. J. Geochem. Explor. 30, 223–242.
Grunsky, E.C., 1986. Recognition of alteration in volcanic rocks using statistical analysis of lithogeochemical data. In: Nichols, C.E. (Ed.), Exploration for Ore Deposits of the North American Cordillera. J. Geochem. Explor. 25, pp. 157–185.
Grunsky, E.E., 2010. The interpretation of geochemical survey data. Geochem. Explor. Environ. Anal. 10, 27–74.
Hall, G.E.M., Bonham-Carter, G.F., Buchar, A., 2014. Evaluation of portable X-ray fluorescence (pXRF) in exploration and mining: phase 1, control reference materials. Geochem. Explor. Environ. Anal. 14, 99–123.
Inverno, C.M.C., Hutchinson, R.W., 2006. Petrochemical discrimination of evolved granitic intrusions associated with Mount Pleasant deposits, New Brunswick, Canada. Trans. Inst. Min. Metall. Sect. B 115, 23–39.
Jenner, G.A., 1996. Trace element geochemistry of igneous rocks: geochemical nomenclature and analytical geochemistry. In: Wyman, D.A. (Ed.), Trace element geochemistry

of volcanic rocks: applications for massive sulphide exploration. Geol. Assoc. Can., Short Course Notes 12, pp. 51–78.
Jolliffe, I.T., 2002. Principal Component Analysis. second ed. Springer, New York, NY (487 pp.).
Kaiser, H.F., 1960. The application of electronic computers to factor analysis. Educ. Psychol. Meas. 20, 141–151.
Kerrich, R., Wyman, D.A., 1996. The trace element systematics of igneous rocks in mineral exploration: an overview. In: Wyman, D.A. (Ed.), Trace Element Geochemistry of Volcanic Rocks: Application for Massive Sulphide Exploration. Geol. Assoc. Can., Short Course Notes 12, pp. 1–50.
Kooiman, G.J.A., McLeod, M.J., Sinclair, W.D., 1986. Porphyry tungsten-molybdenum orebodies, polymetallic veins and replacement bodies, and tin-bearing greisen zones in the Fire Tower Zone, Mount Pleasant, New Brunswick. Econ. Geol. 81, 1356–1373.
Leitch, C.H.B., Lentz, D.R., 1994. The Gresens' approach to mass balance constraints of alteration systems: methods, pitfalls, examples. In: Lentz, D.R. (Ed.), Alteration and Alteration Processes Associated With Ore-forming Systems. Geol. Assoc. Can., Short Course Notes 11, pp. 161–192.
Lentz, D.R., 1996a. Recent advances in lithogeochemical exploration for massive sulphide deposits in volcano-sedimentary environments: petrogenetic, chemostratigraphic, and alteration aspects with examples from the Bathurst Camp, New Brunswick. In: Carroll, B.M. (Ed.), Current Research 1995. New Brunswick Department of Natural Resources and Energy Division, Mineral Resource Report. Vol. 96-1, pp. 73–119.
Lentz, D.R., 1996b. Trace-element systematics of felsic volcanic rocks associated with massive sulphide deposits in the Bathurst Mining Camp, petrogenetic, tectonic and chemostratigraphic implications for VMS exploration. In: Wyman, D.A. (Ed.), Trace Element Geochemistry of Volcanic Rocks: Applications of Massive Sulphide Exploration. Geol. Assoc. Can., Short Course Notes 12, pp. 359–402.
MacLean, W.H., Barrett, T.J., 1993. Lithogeochemical techniques using immobile elements. J. Geochem. Explor. 48, 109–133.
McCutcheon, S.R., 1990. The Late Devonian Mount Pleasant Caldera Complex: Stratigraphy, Mineralogy, Geochemistry and Geological Setting of a Sn-W Deposit in Southwestern New Brunswick. (Unpublished Ph.D. thesis). Dalhousie University, Halifax, Nova Scotia (609 pp.).
McCutcheon, S.R., Anderson, H.E., Robinson, P.T., 1997. Stratigraphy and eruptive history of the Late Devonian Mount Pleasant Caldera Complex, Canadian Appalachians. Geol. Mag. 134, 17–36.
McCutcheon, S.R., Reddick, J., McKeen, T., Scott, S., Kociumbas, M., 2012. Technical Report Mount Pleasant property including an updated mineral resource estimate on the North Zone, south western New Brunswick for Adex Mining Inc. Vol. 170. Watts, Griffis and McOuat (pp.).
McCutcheon, S.R., Sinclair, W.D., McLeod, M.J., Boyd, T., Kooiman, G.J.A., 2010. Mount Pleasant Sn-W-Mo-Bi-In deposit. In: Fyffe, L.R., Thorne, K.G. (Eds.), Polymetallic Deposits of Sisson Brook and Mount Pleasant, New Brunswick, Canada, New Brunswick Department of Natural Resources; Lands, Minerals and Petroleum Division, Field Guide No. 3, pp. 37–68.
Pearce, J.A., Harris, N.B.W., Tindle, A.G., 1984. Trace element discrimination diagrams for the tectonic interpretation of granitic rocks. J. Petrol. 25, 956–983.
Piercey, S.J., 2014. A review of quality assurance and quality control (QA/QC) procedures for lithogeochemical data. Geosci. Can. 41, 1–14.
Piercey, S.J., Devine, M.C., 2014. Analysis of powdered reference materials and known samples with a benchtop, field portable X-ray fluorescence (pXRF) spectrometer: evaluation of performance and potential applications for exploration lithogeochemistry. Geochem.: Explor., Environ., Anal. 14, 139–148.
Pouliot, G., Barondeau, B., Sauve, P., Davis, M., 1978. Distribution of alteration minerals and metals in the Fire Tower Zone at Brunswick Tin Mines LTD., Mount Pleasant area, New Brunswick. Can. Mineral. 16, 223–237.
Ragland, P.C., Conley, J.F., Parker, W.C., Van Orman, J.A., 1997. Use of principal components analysis in petrology: an example from the Martinsville igneous complex, Virginia, U.S.A. Mineral. Petrol. 60, 165–184.
Ross, P.S., Bourke, A., Fresia, B., 2014. Improving lithological discrimination in exploration drill-cores using portable X-ray fluorescence measurements: (2) application to the Zn-Cu Matagami mining camp, Canada. Geochem. Explor. Environ. Anal. 14, 187–196.
Rubio, B., Nombela, M.A., Vilas, F., 2000. Geochemistry of major and trace elements in sediments of the Ria de Vigo (NW Spain): an assessment of metal pollution. Mar. Pollut. Bull. 40, 968–980.
Shahi, H., Ghavami, R., Rouhani, A.K., Kahoo, A.R., Haroni, H.A., 2015. Application of Fourier and wavelet approaches for identification of geochemical anomalies. J. Afr. Earth Sci. 106, 118–128.
Shikazono, N., Ogawa, Y., Utada, M., Ishiyama, D., Mizuta, T., Ishikawa, N., Kubota, Y., 2008. Geochemical behavior of rare earth elements in hydrothermally altered rocks of the Kuroko mining area, Japan. J. Geochem. Explor. 98, 65–79.
Sinclair, W.D., Kooiman, G.J.A., 1990. The Mount Pleasant tungsten-molybdenum and tin deposits. In: Boyle, D.R. (Ed.), Mineral Deposits of New Brunswick and Nova Scotia [Field Trip 2], 8th IAGOD Symposium Field Trip Guidebook. Geol. Surv. Can., Open File 2157, pp. 78–87.
Sinclair, W.D., Kooiman, G.J.A., Martin, D.A., 1988. Geological setting of granites and related tin deposits in the North Zone, Mount Pleasant, New Brunswick. Geol. Surv. Can. Curr. Res. B 201–208 (Paper 88-1B).
Sinclair, W.D., Kooiman, G.J.A., Martin, D.A., Kjarsgaard, I.M., 2006. Geology, geochemistry and mineralogy of indium resources at Mount Pleasant, New Brunswick, Canada. Ore Geol. Rev. 28, 123–145.
Taylor, R.P., Sinclair, W.D., Lutes, G., 1985. Geochemical and isotopic characterization of granites related to W-Sn-Mo mineralization in the Mount Pleasant area, New Brunswick. In: Taylor, R.P., Strong, D.F. (Eds.), Granite - Related Mineral Deposits - Geology, Mineralogy and Paragenesis, Extended Abstracts of Papers. The Canadian Institute of Mining and Metallurgy Conference, Halifax, Nova Scotia, pp. 265–273.
Thompson, M., Howarth, R.J., 1973. The rapid estimation and control of precision by duplicate determinations. Analyst 98, 153–160.
Thorne, K.G., Fyffe, L.R., Creaser, R.A., 2013. Re-Os geochronological constraints on the W-Mo mineralizing event in the Mount Pleasant Caldera Complex: implications for the timing of subvolcanic magmatism and caldera development. Atl. Geol. 49, 131–150.
Tucker, R.D., Bradley, D.C., ver Straeten, C.A., Harris, A.C., Ebert, J.R., McCutcheon, S.R., 1998. New U-Pb zircon ages and the duration and division of Devonian time. Earth Planet. Sci. Lett. 158, 175–186.
USEPA (United States Environmental Protection Agency), 2007. Method 6200. Field portable X-ray fluorescence spectrometry for the determination of elemental concentrations in soil and sediment. Revision 0. February 2007 http://www.epa.gov/wastes/hazard/testmethods/sw846/pdfs/6200.pdf Washington, D.C.
Vaillant, M.L., Barnes, S.J., Fisher, L., Fiorentini, M.L., Caruso, S., 2014. Use and calibration of portable X-ray fluorescence analysers: application to lithogeochemical exploration for komatiite-hosted nickel sulphide deposits. Geochem. Explor. Environ. Anal. 14, 199–209.
Wang, C.M., Carranza, E.J.M., Zhang, S.T., Zhang, J., Liu, X.J., Zhang, D., Sun, X., Duan, C.J., 2013. Characterization of primary geochemical halos for gold exploration at the Huanxiangwa gold deposit, China. J. Geochem. Explor. 124, 40–58.
Wang, W.L., Zhao, J., Cheng, Q.M., 2014. Mapping of Fe mineralization-associated geochemical signatures using log ratio transformed stream sediment geochemical data in eastern Tianshan, China. J. Geochem. Explor. 141, 6–14.
Yang, X.M., Lentz, D.R., McCutcheon, S.R., 2003. Petrochemical evolution of subvolcanic granitoid intrusions within the Late Devonian Mount Pleasant Caldera, southwestern New Brunswick, Canada: comparison of Au versus Sn-W-Mo-polymetallic mineralization systems. Atl. Geol. 39, 97–121.
Zhang, W., Lentz, D.R., 2016. Application of portable X-ray fluorescence analyses to discriminate rock units in the Fire Tower Zone, Mount Pleasant Deposit, New Brunswick. New Brunswick Department of Energy and Mines, Geological Surveys Branch, Geoscience Report 2016-1 (25 pp.).
Zuo, R.G., 2011. Identifying geochemical anomalies associated with Cu and Pb-Zn skarn mineralization using principal component analysis and spectrum-area fractal modeling in the Gangdese Belt, Tibet (China). J. Geochem. Explor. 111, 13–22.